Title

Trace gas transport and scavenging in PEM-Tropics B South Pacific Convergence Zone convection

Journal

Journal of Geophysical Research, 106(D23)

ISSN

0148-0227

Authors

Pickering, Kenneth E
Thompson, Anne M
Kim, Hyuncheol
et al.

Publication Date

2001-12-16

DOI

10.1029/2001jd000328

JOURNAL OF GEOPHYSICAL RESEARCH, VOL. 106, NO. D23, PAGES 32,591–32,602, DECEMBER 16, 2001

Trace gas transport and scavenging in PEM-Tropics B South Pacific Convergence Zone convection

Kenneth E. Pickering,[1] Anne M. Thompson,[2] Hyuncheol Kim,[1] Alex J. DeCaria,[1,3] Leonhard Pfister,[4] Tom L. Kucsera,[5] Jacquelyn C. Witte,[5] Melody A. Avery,[6] Donald R. Blake,[7] James H. Crawford,[6] Brian G. Heikes,[8] Glen W. Sachse,[6] Scott T. Sandholm,[9] and Robert W. Talbot[10]

Abstract. Analysis of chemical transport on Flight 10 of the 1999 Pacific Exploratory Mission (PEM) Tropics B mission clarifies the role of the South Pacific Convergence Zone (SPCZ) in establishing ozone and other trace gas distributions in the southwestern tropical Pacific. The SPCZ is found to be a barrier to mixing in the lower troposphere but a mechanism for convective mixing of tropical boundary layer air from northeast of the SPCZ with upper tropospheric air arriving from the west. A two-dimensional cloud-resolving model is used to quantify three critical processes in global and regional transport: convective mixing, lightning NO_x production, and wet scavenging of soluble species. Very low NO and O_3 tropical boundary layer air from the northeastern side of the SPCZ entered the convective updrafts and was transported to the upper troposphere where it mixed with subtropical upper tropospheric air containing much larger NO and O_3 mixing ratios that had arrived from Australia. Aircraft observations show that very little NO appears to have been produced by electrical discharges within the SPCZ convection. We estimate that at least 90% of the HNO_3 and H_2O_2 that would have been in upper tropospheric cloud outflow had been removed during transport through the cloud. Lesser percentages are estimated for less soluble species (e.g., <50% for CH_3OOH). Net ozone production rates were decreased in the upper troposphere by ~60% due to the upward transport and outflow of low-NO boundary layer air. However, this outflow mixed with much higher NO air parcels on the southwest edge of the cloud, and the mixture ultimately possessed a net ozone production potential intermediate between those of the air masses on either side of the SPCZ.

1. Introduction

The South Pacific Convergence Zone (SPCZ) is one of the Earth's most expansive and persistent convective cloud bands and plays an important role in global circulation patterns. Although this meteorological feature was first noted in the 1930s, it was not until *Trenberth* [1976] designated it as the SPCZ that this term came into common usage. Results from the Pacific Exploratory Mission (PEM) Tropics A field mission [*Gregory et al.*, 1999] suggested that the SPCZ acts as a barrier between the tropical and subtropical air masses of the western South Pacific, particularly at lower tropospheric levels. PEM-Tropics B [*Raper et al.*, this issue] took place at a time of year (March) when the SPCZ is more well defined than during the September period of PEM-Tropics A. The SPCZ was in close proximity to Fiji during PEM-Tropics B. Therefore a flight of the DC-8 from Fiji (Flight 10 on March 20–21, 1999) was designed to sample the air in and around the SPCZ. During this flight, profiles from the boundary layer to ~11 km were performed on both sides of the SPCZ, and two upper tropospheric passes through the SPCZ were flown. In addition, the DC-8 flew through a weaker band of convection located to the north of the SPCZ. The meteorological and chemical measurements conducted on board the DC-8 allow us to perform an analysis of transport and scavenging in the deep convection. In addition, the measurements provide data to initialize and evaluate a cloud-resolving model simulation of a representative cell in the SPCZ convection. We use the model and associated chemical tracer transport calculations along with the observed data to examine convective transport, lightning NO_x production, and wet scavenging in the SPCZ. Analysis of the chemical data along with the tracer simulation has allowed us to characterize the mechanism of convective mixing of the tropical and subtropical air masses.

A large, persistent convective system such as the SPCZ is likely to have substantial effects on tropospheric chemistry.

[1]Department of Meteorology, University of Maryland, College Park, Maryland, USA.
[2]Laboratory for Atmospheres, NASA Goddard Space Flight Center, Greenbelt, Maryland, USA.
[3]Now at Department of Earth Sciences, Millersville University, Millersville, Pennsylvania, USA.
[4]NASA Ames Research Center, Moffitt Field, California, USA.
[5]Science Systems and Applications, Inc., NASA Goddard Space Flight Center, Greenbelt, Maryland, USA.
[6]NASA Langley Research Center, Hampton, Virginia, USA.
[7]Department of Chemistry, University of California, Irvine, California, USA.
[8]Graduate School of Oceanography, University of Rhode Island, Narragansett, Rhode Island, USA.
[9]School of Earth and Atmospheric Sciences, Georgia Institute of Technology, Atlanta, Georgia, USA.
[10]Institute for Earth, Oceans, and Space, University of New Hampshire, Durham, New Hampshire, USA.

Paper number 2001JD000328.
0148-0227/01/2001JD000328$09.00

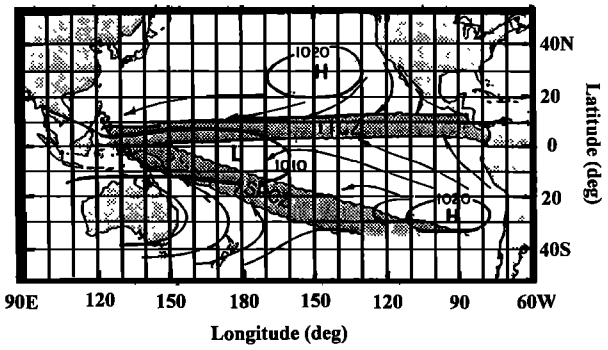

Figure 1. Schematic of relationship of SPCZ and ITCZ showing mean annual sea level pressure and surface wind streamlines [from *Trenberth*, 1991]. Reprinted with the permission of Cambridge University Press.

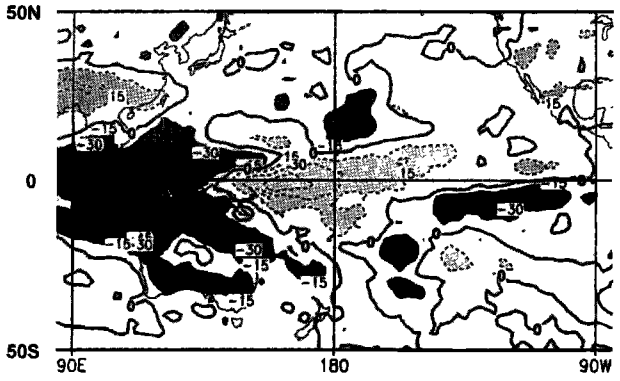

Figure 2. Mean anomaly in outgoing longwave radiation for March 1999. Contour interval is 15 W m^{-2} with positive values indicated by dashed contours and light shading. Measurements taken by NOAA 12 AVHRR instrument. Anomalies are departures from mean of March 1979–1995 [from *Climate Prediction Center*, 1999].

Deep convection has been shown in numerous studies [e.g., *Dickerson et al.*, 1987; *Pickering et al.*, 1990, 1996] to be effective at rapidly transporting boundary layer air to the upper troposphere. As a result, free tropospheric ozone production is perturbed due to the convectively induced changes in NO_x and HO_x. Over the remote oceans, marine boundary layer air with low NO_x and low O_3 mixing ratios is transported upward by deep convection [e.g., *Pickering et al.*, 1993] tending to decrease the magnitude of ozone production in the upper troposphere. *Lelieveld and Crutzen* [1994] suggested that convection over the remote oceans tends to bring higher values of NO_x and O_3 down to the boundary layer where their lifetimes are relatively short, thereby causing a decrease in tropospheric ozone. Although lightning is much less frequent in marine convection than in continental storms [e.g., *Christian and Latham*, 1998], significant perturbations to NO_x have been noted in association with marine storms [e.g., *Chameides et al.*, 1987]. The large amounts of liquid water in tropical convection may efficiently remove soluble gases and aerosols from the atmosphere. The results of transport, lightning, and scavenging analyses for the observed SPCZ convection will increase our understanding of these processes over the tropical oceans and will contribute to improvements in parameterizations of them in global chemical transport models.

Section 2 of the paper provides background material on the climatology of the SPCZ and the meteorology of the SPCZ for the PEM-Tropics B convective event that was sampled by the DC-8 and simulated with the cloud model. Section 3 presents the DC-8 meteorological and chemical measurements from the SPCZ flight, and section 4 details our cloud model analysis. In section 5 we discuss our results in relation to previous work, and section 6 summarizes the findings of our analyses.

2. SPCZ Meteorology

2.1. Climatology

The SPCZ is a zone of primarily low-level convergence consisting of a zonal portion to the northwest of New Guinea where it joins with the Intertropical Convergence Zone (ITCZ) and a diagonal portion which extends southeastward from New Guinea to approximately 30°S and 150°W (see schematic in Figure 1). It is most well-defined in January and February; therefore the PEM-Tropics B field mission of March and early April occurred after the typical time of maximum intensity. A thorough review of the characteristics of the SPCZ, its origin and maintenance, and its significance in the global circulation has been published by *Vincent* [1994]. *Streten* [1973] found through analysis of satellite imagery that the SPCZ contained a higher percentage cloud cover than any other region of the Southern Hemisphere. These values maximize in the Southern Hemisphere summer, along with the synoptic-scale vertical velocity. At this time of year there is also a minimum in outgoing longwave radiation in the SPCZ. *Kiladis et al.* [1989] have shown that maximum surface wind convergence in the SPCZ occurs south of the axis of maximum precipitation and the maximum precipitation lies south of the region of maximum sea surface temperature. *Huang and Vincent* [1983] showed that the sea level pressure trough associated with the SPCZ lies along the southwest edge of the SPCZ cloud band. This arrangement suggests that the deep convection forms primarily in the tropical air to the north of the convergence zone. We employ this concept in section 4 when we select a profile for initializing the cloud model simulation.

The zonal portion of the SPCZ may be maintained due to the "warm pool" of seawater in this region. The sea surface temperature gradients may force the low-level winds [e.g., *Lindzen and Nigam*, 1987] resulting in convergence. The diagonal portion of the SPCZ, which is the portion near Fiji, results from a tropical-midlatitude interaction. The convergence zone results from the northeasterly flow on the northwest side of the subtropical eastern Pacific high and the slightly cooler and drier southeasterly flow from the subtropical latitudes of the Southern Hemisphere located farther to the south and west. This convergence zone interacts with transient troughs in the midlatitude westerlies. The frontal activity associated with these troughs strengthens the convergence between them and the subtropical high. The fronts in the westerlies propagate equatorward from near New Zealand and often become quasistationary in the SPCZ.

Fuelberg et al. [this issue] summarized positions of the SPCZ for each PEM-Tropics B flight. Greater variability in the position was noted in the far southeast portion of the SPCZ due to the influence of midlatitude cyclones and cold fronts. The fronts moved to the northeast and became stationary at 15°–20°S. The convergence associated with the front became connected with the SPCZ. Figure 2 shows the anomaly field for outgoing longwave radiation for March 1999. While strong

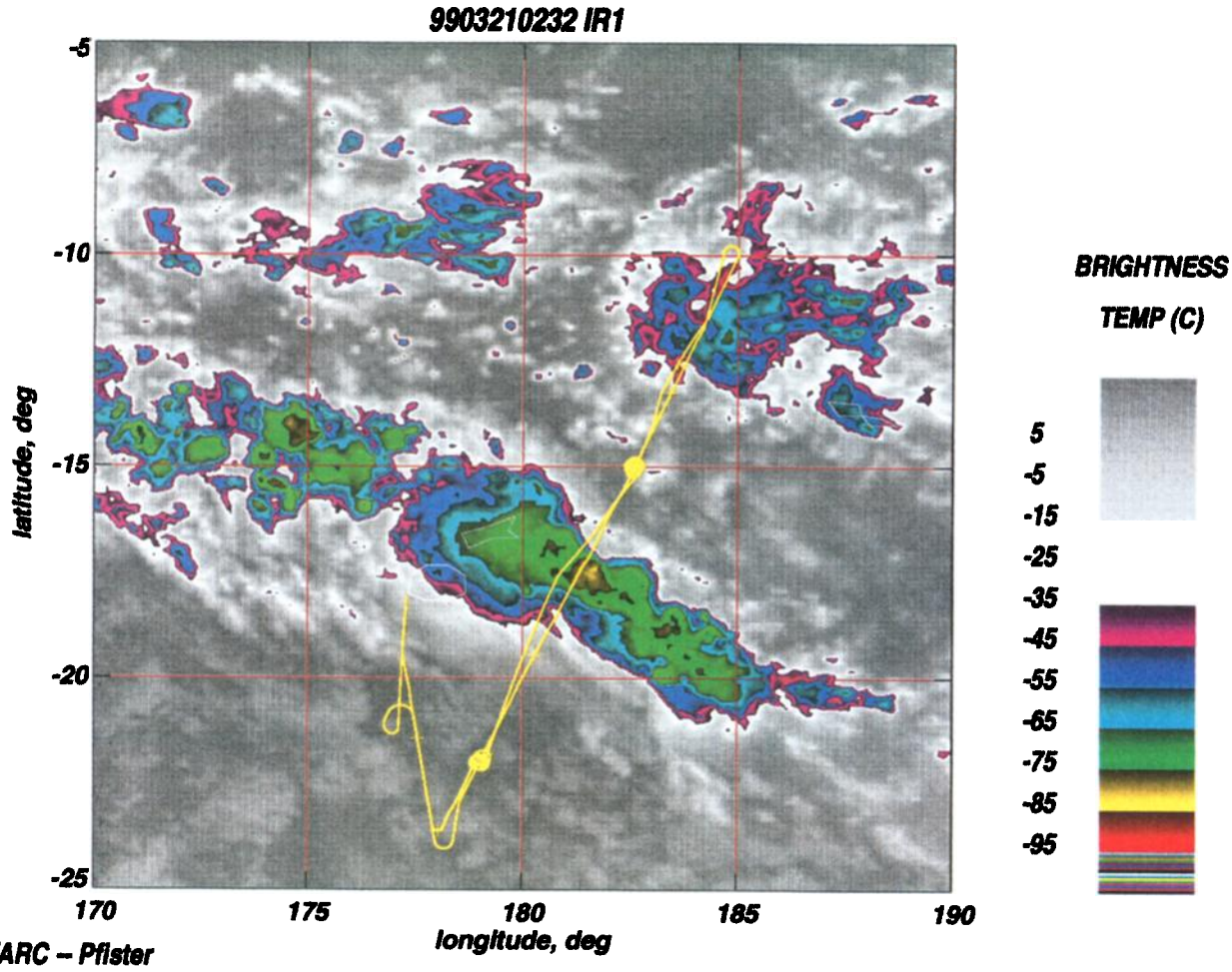

Plate 1. Color-enhanced IR image from GMS satellite at 0232 UT March 21, 1999. NASA DC-8 flight track is superimposed using yellow line.

negative anomalies (implying more frequent or deeper convection than normal) existed at the western end of the SPCZ and strong positive anomalies (implying less convection than normal) are seen to the east, the anomaly was near zero in the vicinity of Fiji. Therefore it appears that the strength of the SPCZ convection near Fiji in March 1999 was near normal. The anomalies noted are related to the La Niña conditions that existed in 1999. While the SPCZ convection near Fiji appeared near normal, the transport characteristics of the region may not have been normal due to the strong anomalies in convection to the east and west.

2.2. Meteorology of SPCZ Convection of March 20–21, 1999

On March 21, 1999, the SPCZ was located just north of Fiji as seen in Plate 1, which is an infrared cloud image from the GMS satellite at 0232 UT. The flight track of the DC-8 aircraft is superimposed on the image. After takeoff from Fiji, the aircraft sampled air on the southwest side of the SPCZ. It then passed through the SPCZ convective cloud band at 10.7 km and continued to the northeast where weaker convection was sampled at 8.8 to 11.3 km. The plane turned around at ~10°S and descended through the weaker cloud band, reaching the boundary layer on the southwest side. The marine boundary layer on the northeast side of the SPCZ was sampled for about 20 min prior to an ascending spiral to 11.3 km. The aircraft then passed through the SPCZ at this altitude, followed by a descending spiral to the boundary layer on the southwest side of the SPCZ convection prior to the return to Fiji.

Plate 2 shows the evolution of the minimum cloud top pressures of the SPCZ convection from 2100 UT on March 20 to 0425 UT on March 21. The SPCZ convective activity near Fiji intensified around 0900 on March 20. By 2100 UT (Plate 2a) a strong cell with cloud top of ~115 hPa was located just northeast of Fiji. This cell had intensified further by 2225 UT (Plate 2b), when the DC-8 took off from Fiji. The cell weakened by 0000 UT March 21, allowing the DC-8 to pass near it during the northbound traverse of the SPCZ. By 0132 UT (Plate 2d), very deep convection extended well to the southeast in a rather solid line. However, by 0300 UT the line became less intense except for one cell at ~178°W. The DC-8 passed just west of this cell during its southbound SPCZ traverse. The very deep SPCZ convection persisted to the southeast of Fiji until ~1500 UT. The coldest cloud tops during this period in the flight region were at approximately 105 hPa, or ~16 km.

Figure 3 shows plots of the ECMWF wind vector field for several levels in the atmosphere at 0000 UT March 21. At 1000 and 950 hPa, NE winds were present northeast of the SPCZ, and SE winds existed on the southwest side. This low-level

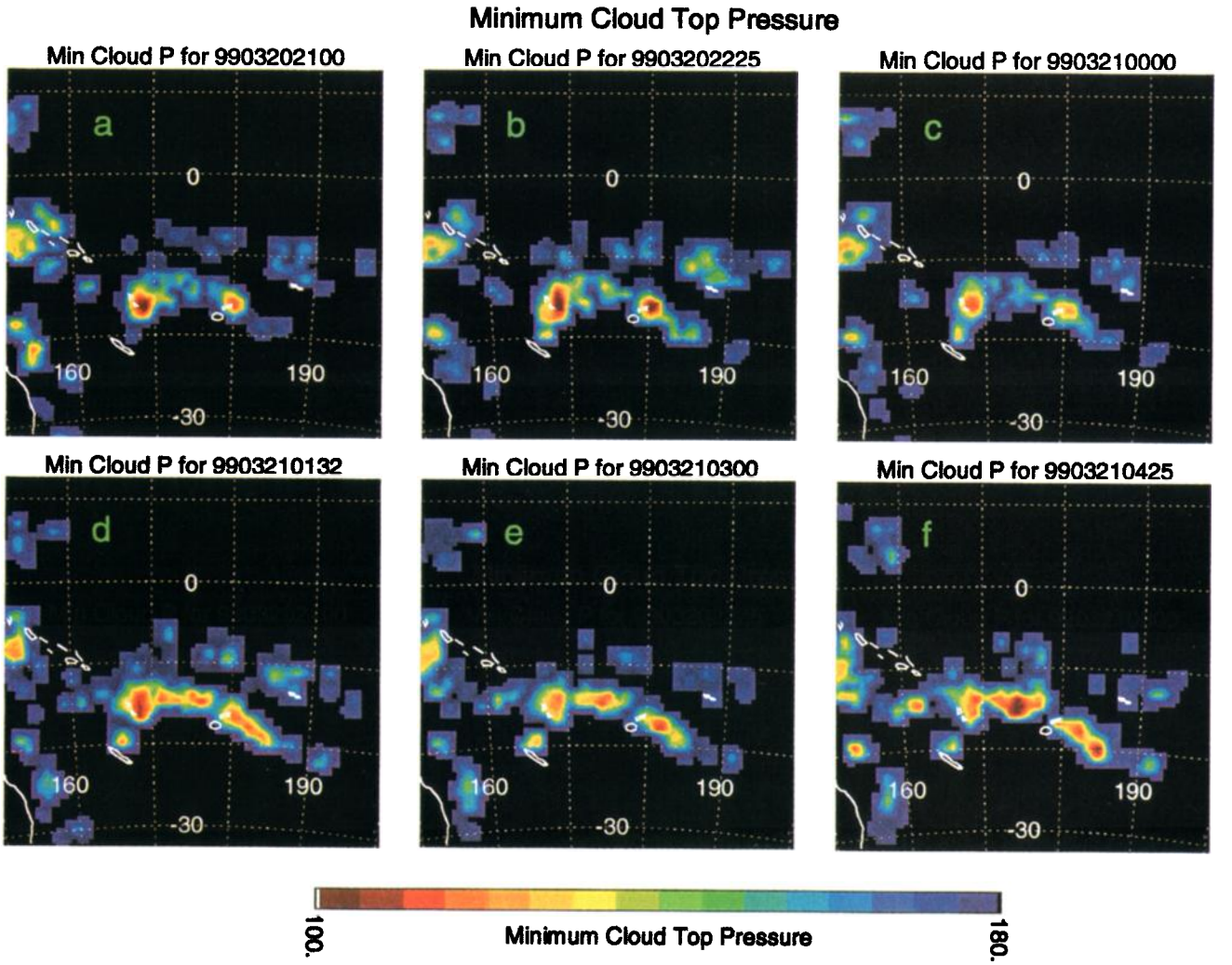

Plate 2. Minimum cloud top pressures (hPa) for clouds with tops at <180 hPa, derived from GMS IR images at (a) 2100 UT March 20; (b) 2225 UT March 20; (c) 0000 UT March 21; (d) 0132 UT March 21; (e) 0300 UT March 21; and (f) 0425 UT March 21, 1999. Minimum cloud top pressures are determined by finding the pixel with the coldest IR brightness temperature within each 1° × 1° grid cell. The pressure level having this temperature is then determined from the NASA Data Assimilation Office's gridded global analysis.

convergence was strongest along a line from ~13°S, 170°E to ~20°S, 170°W. At low levels, air approached the northeast side of the SPCZ near Fiji after a long transit across the Pacific at tropical latitudes of the Southern Hemisphere. On the southwest side, air approached from the southeast. Therefore it appears that in the vicinity of Fiji the SPCZ represented a convergence zone for two Southern Hemispheric air masses. However, well to the northwest of Fiji the tropical air approaching the SPCZ had a Northern Hemispheric origin. There the SPCZ is a line of convergence of air masses from the two hemispheres.

At 500 hPa there were easterly winds on the northeast side of the SPCZ and northwesterly winds on the southwest side. At higher levels the westerlies were relatively strong southwest of the SPCZ, while easterlies still prevailed to the northeast of the SPCZ.

3. Measurements

In this section we describe the set of measurements taken by the DC-8 near and within the SPCZ on March 20–21, 1999. A complete listing of all the chemical species that were measured, along with the techniques, averaging times, accuracy, precision, and limits of detection is provided by *Raper et al.* [this issue].

3.1. Profiles

Plate 1 shows that spiral profiles (yellow dots) were flown by the DC-8 on the north and south sides of the SPCZ. *Fuelberg et al.* [this issue] present the temperature, moisture, and wind profiles observed during the ascent (northeast side) and descent (southwest side). Northeast of the SPCZ there were no temperature inversions on the profile, while on the south side a strong inversion was present based at ~730 hPa. Above this inversion, likely caused by subsidence, was much drier air. The middle and upper troposphere were much more moist on the northeast side of the SPCZ. Near the surface the air northeast of the SPCZ was warmer and more moist than southwest of the SPCZ.

Figures 4a and 4b show the O_3 and CO profiles observed on the northeast and southwest side of the SPCZ, respectively. Much lower O_3 was found on the northeast side, with near-surface values as low as 5–7 ppbv; and in the free troposphere, O_3 was typically 12–17 ppbv. These boundary layer values were

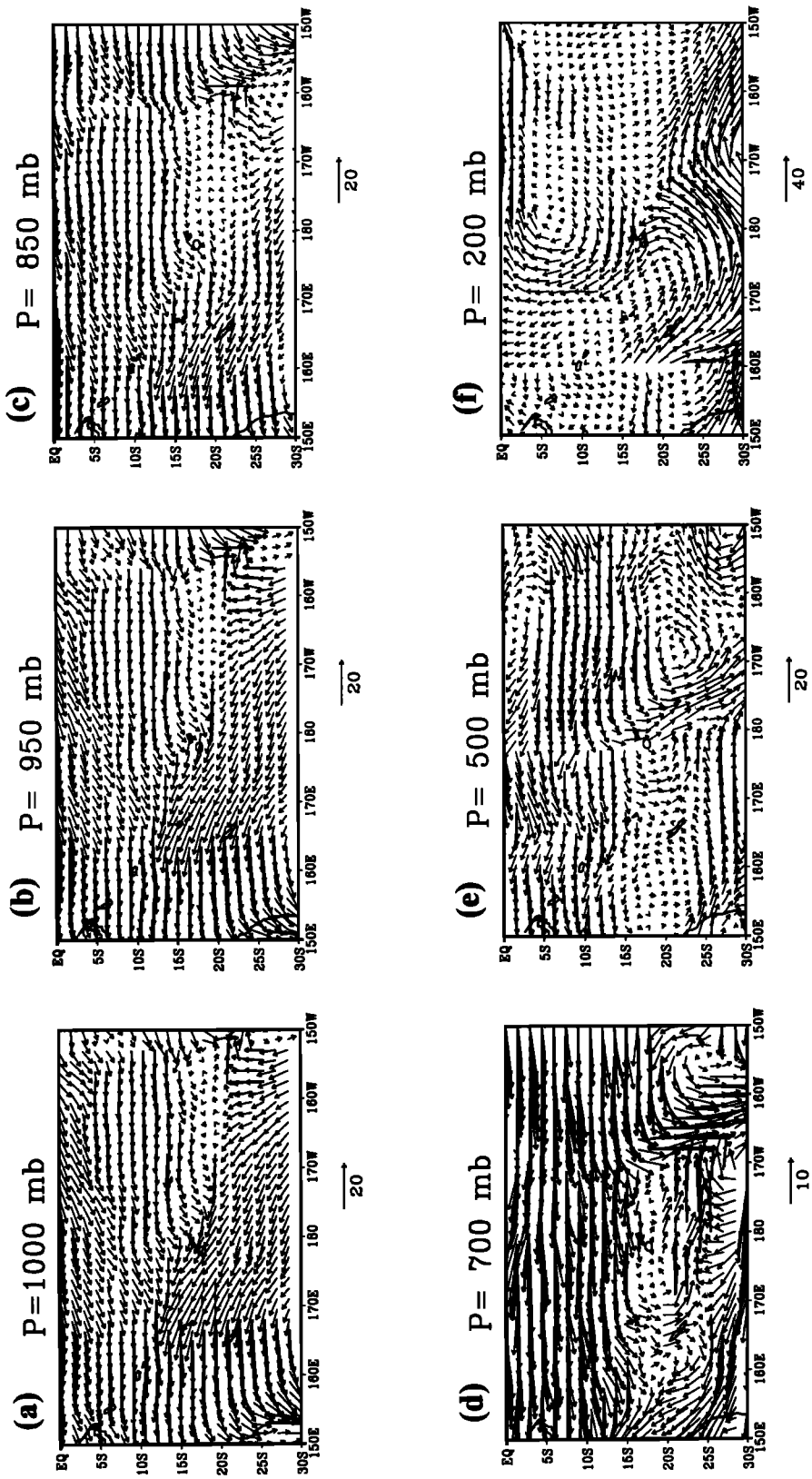

Figure 3. Wind fields from ECMWF analyses at 0000 UT March 21, 1999. Fields have horizontal resolution of 1.5° × 1.5°. Length of vector beneath each plot signifies given wind speed. Winds are given at (a) 1000 hPa; (b) 950 hPa; (c) 850 hPa; (d) 700 hPa; (e) 500 hPa; and (f) 200 hPa.

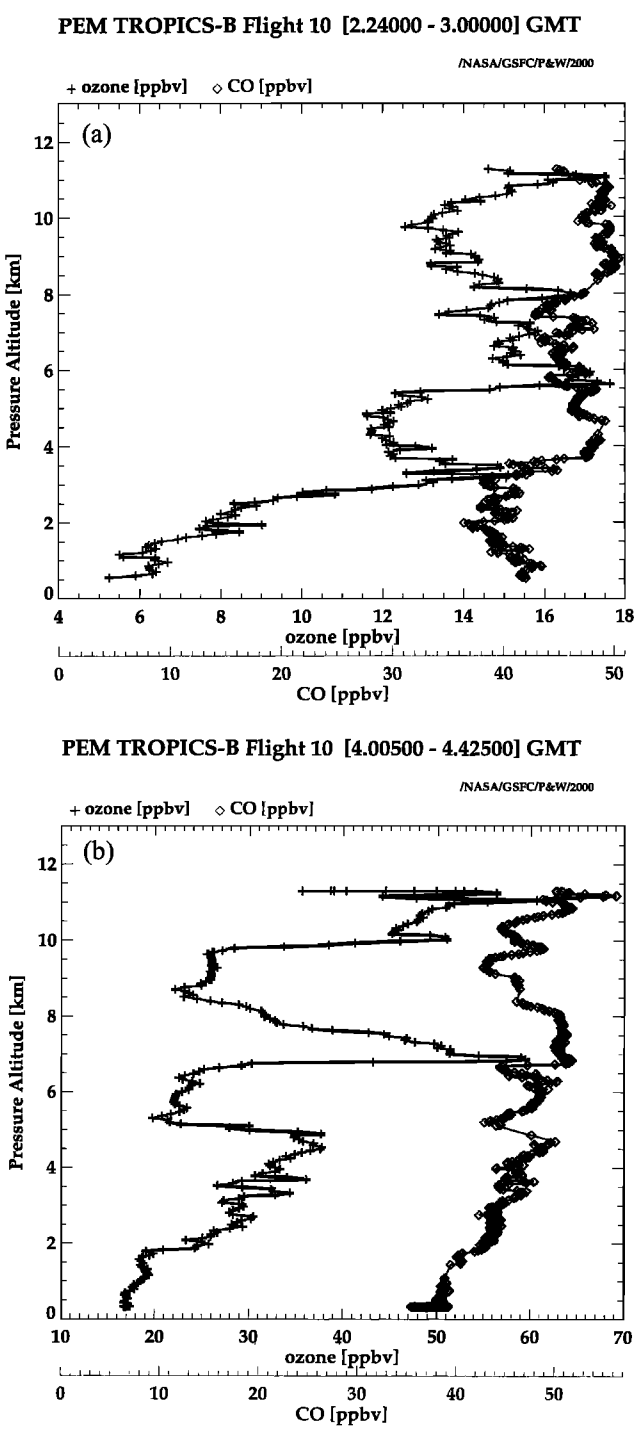

Figure 4. Profiles of O_3 and CO measured on the DC-8 during (a) spiral northeast of the SPCZ and (b) spiral southwest of the SPCZ. See Plate 1 for locations.

some of the smallest measured during PEM-Tropics B and result from the long fetch of the northeasterly winds with ozone being destroyed at the ocean surface during transport. In contrast, boundary layer O_3 on the southwest side was 17–19 ppbv with lower free troposphere values of 20–35 ppbv. In addition, two pronounced O_3 plumes were found on the southwest side. The upper plume with maximum ozone of ~60 ppbv was located in the 10–11.3 km layer. The lower plume was in the 6.5–8 km layer and also reached a maximum of ~60 ppbv. Convective influence trajectory analysis was conducted by running isentropic back trajectories from all points on a 1° latitude by 1° longitude array over the PEM-Tropics B region and determining which of these trajectories intersected deep convective clouds on a series of infrared satellite images [*Thompson et al.*, 2000]. Figure 5 shows back trajectories indicating that air arriving on the southwest side of the SPCZ at ~11 km likely consisted of outflow from deep convection over northern Australia 3 days earlier (March 18). This convection was evidently associated with lightning flashes detected by the Lightning Imaging Sensor (LIS [*Christian et al.*, 1999]) on board the Tropical Rainfall Measuring Mission (TRMM) during its March 18 pass over northeast Australia.

Figure 6 shows the NO_x and HNO_3 profiles on both sides of the SPCZ. The northeast side of the SPCZ was characterized by very small mixing ratios of NO_x (Figure 6a). On the southwest side a NO_x plume of ~50 to 75 pptv in the same layer as the upper ozone plume may signify that lightning NO_x catalyzed ozone production during the 3 days transport from Australia. Little nitric acid (Figure 6d) and hydrogen peroxide were found in this plume, supporting an interpretation of convective outflow following scavenging. In the lower altitude ozone plume (~7 km altitude) there was little NO_x, but substantial plumes of nitric acid (up to ~275 pptv), H_2O_2, and PAN were observed. This could suggest a nonconvective origin (no wet scavenging) or that the source of the plume was located further back in time than for the upper plume, allowing more conversion of NO_x to nitric acid and PAN. In addition, a small enhancement in CO (~6 ppbv) was also evident. Figure 7 shows a cluster of 10-day back trajectories for the lower altitude ozone plume. The majority of these trajectories passed over southern Australia 4 to 5 days back in time. A frontal system with moderate cloud tops (7–9 km) crossed southern Australia during these 2 days. Polluted air may have been lofted ahead of the cold front followed by photochemical processing during transport.

Figure 8 shows very sharp gradients of CH_3I, a tracer of marine origins [*Davis et al.*, 1996a; *Cohan et al.*, 1999] within the boundary layer. On the northeast side of the SPCZ, mixing ratios decreased with altitude from 0.47 pptv at 0.4 km to <0.2 pptv at 1 km. Boundary layer values were larger on the southwest side of the SPCZ, decreasing with altitude from 0.72 pptv at 0.3 km. Mixing ratios remained >0.2 pptv at all altitudes below 2 km. These boundary layer maxima allow CH_3I to be an excellent tracer of marine convective transport from the boundary layer to the free troposphere as demonstrated in the following subsection.

3.2. Observed Trace Gases During Transects of the SPCZ

Figures 9a and 9b show CO and O_3 observed during the northbound and southbound passages of the DC-8 through the SPCZ. Owing to the fact that smaller mixing ratios of CO and O_3 existed in the marine boundary layer (e.g., 38–42 ppbv CO and 6 ppbv O_3 from Figure 4a) than aloft in the air mass in which the SPCZ convection developed, low values of these species during the SPCZ crossing at ~11 km indicate convective outflow. During the northbound (first) SPCZ crossing, ozone reached a minimum of 12–13 ppbv in the outflow, compared with 14–17 ppbv in undisturbed air at ~11 km. CO reached minima of 44 and 47 ppbv, compared with 47–51 ppbv in undisturbed air. Therefore, because the observed minima at ~11 km were not as small as the boundary layer mixing ratios, it appears that significant mixing and dilution occurred during

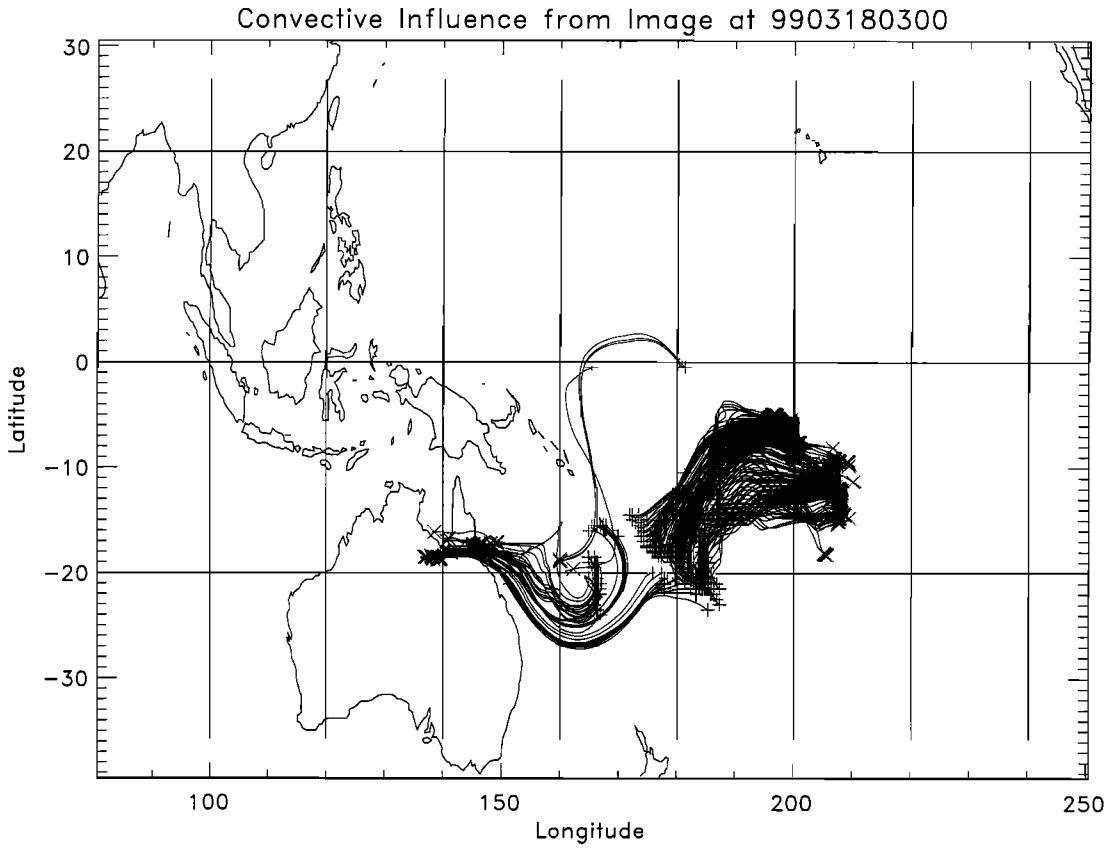

Figure 5. Trajectories on 345 K isentropic surface which extend backward from set of points (pluses) to deep convective cloud locations (crosses) determined from satellite imagery. Trajectories initialized at 0200 UT March 21, 1999, and cloud locations derived from IR image at 0300 UT March 18, 1999.

the convective transport. The aircraft passed just east of the dominant cell in this section of the SPCZ. However, with easterly winds at flight level, it is unlikely that the maximum effect of the convection was sampled during this crossing. During the southbound (second) SPCZ crossing, sudden decreases of ozone and CO to minima of 10 ppbv and 40–42 ppbv, respectively, were noted. It appears that little mixing of the cloud outflow with the upper tropospheric air arriving from the east had occurred on the northeastern edge of the cloud band. In this case the aircraft passed just to the west of the dominant cell. Therefore it is not surprising that more pronounced minima in ozone and CO were noted (0320–0324 UT) than during the first SPCZ crossing. Following these minima, both CO and O_3 gradually increased as the DC-8 approached the southwestern edge of the convective band. At 0335 UT the winds shifted from easterly to westerly near the edge of the cloud, and by 0350 UT the air with much larger ozone mixing ratios on the southwest side of the SPCZ was encountered. Therefore the region between the maximum convective outflow (~0324 UT) and the subtropical air (~0350 UT) represents a zone of mixing of tropical marine boundary layer air with air in the subtropical upper troposphere.

Figure 10 presents the observations of CH_3I taken during the SPCZ traverses. Maximum values of CH_3I mixing ratio correspond closely in time with the ozone minima. These maxima reached 0.28 pptv during the northbound crossing and 0.36 to 0.40 pptv in the more intense convective outflow encountered during the southbound crossing. Minimum values of O_3 and maximum values of CH_3I noted during the SPCZ crossings suggest that most of the air entrained into the SPCZ convection derived from the northeast side of the convective system. If substantial boundary layer air from the southwest side of the SPCZ had entered the system, the pronounced ozone minima would not have been found in the convective outflow, and the CH_3I values would have been larger. This result is in agreement with climatological analyses (see section 2.1) which indicate that the SPCZ convection typically develops in the tropical air on the northern edge of the zone of convergence. Figure 11 shows the mixing ratios of NO_x and HNO_3 during the SPCZ crossings. NO_x mixing ratios dropped to as low as 10 pptv during the southbound traverse. HNO_3, which is an extremely soluble gas, was substantially depleted, especially during the southbound crossing. Values as low as 5 pptv of HNO_3 were measured.

4. Model Analyses

The observations discussed in section 3 provide information on the net effect of several processes associated with convective clouds. In combination with a cloud model, the observations can yield further information concerning the individual processes of convective transport, wet scavenging of soluble species, and production of NO_x by lightning.

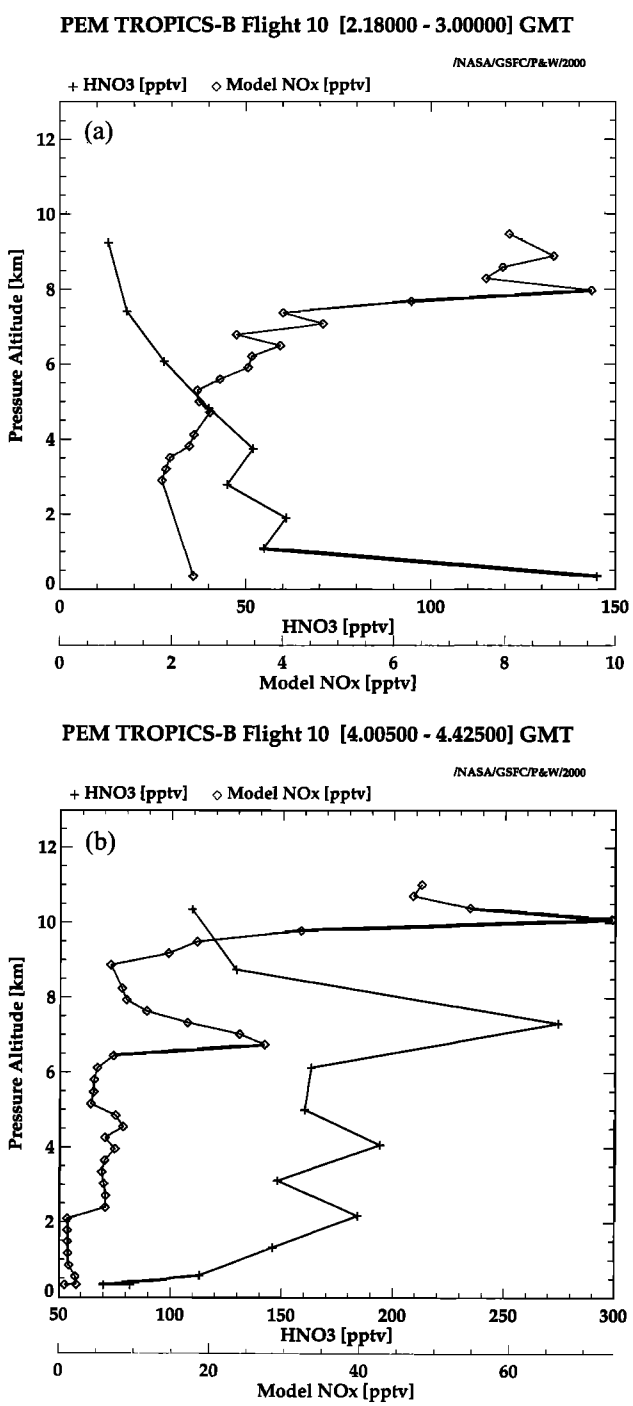

Figure 6. Profiles of HNO_3 measured on the DC-8 and NO_x computed from the Langley/GIT box model for (a) spiral northeast of the SPCZ and (b) spiral southwest of the SPCZ. See Plate 2 for locations.

4.1. Two-Dimensional Goddard Cumulus Ensemble (GCE) Model

The GCE model has been used extensively for studies of convective transport of trace gases in both the tropics and midlatitudes [e.g., *Scala et al.*, 1990; *Pickering et al.*, 1991, 1992, 1996, 1998; *Stenchikov et al.*, 1996; *DeCaria et al.*, 2000]. Here we use the model to investigate trace gas transport in a representative convective system in the SPCZ near Fiji.

A complete description of the GCE model and its governing equations is given by *Tao and Simpson* [1993]. The model uses a parameterized Kessler-type liquid water scheme [*Kessler*, 1969] for cloud and rainwater and a parameterized ice phase scheme for cloud ice, snow, and hail/gaupel [*Lin et al.*, 1983]. The two-dimensional (2-D) version of the model in use at the University of Maryland does not include radiative transfer processes because they are not significant on the several-hour timescale of the simulations conducted in this study [*Tao et al.*, 1993].

A uniform vertical grid extending to ~24 km with spacing of 0.33 km is used. There are 514 horizontal grid points with the center 430 having a fine resolution of 1 km. The outer grid points are stretched horizontally, and open lateral boundary conditions are used. The horizontal axis of the model was oriented east-west because the airflow was primarily in this direction. The simulation was run for a 5-hour period. We initiate convection by artificially heating a shallow layer near the surface to create a "warm bubble" during the first 10 min of simulation.

4.2. Initial Conditions

Figure 12 shows the profiles of temperature, moisture, and winds that were used to initialize the 2-D GCE model. These profiles were primarily derived from the DC-8 profile northeast of the SPCZ because the low-level air was warmer and more moist and therefore more conducive for convective cloud development than was the air on the southwest side. In addition, the chemical data suggested that it was the tropical air mass that was entrained into the cloud system. The sounding used in the model had convective available potential energy (CAPE) of 2086 J kg^{-1}, which is fairly substantial for marine convective environments, but considerably less than the CAPE that often develops over continents. Above the highest DC-8 altitude (~11 km) the profiles were constructed from European Centre for Medium-Range Weather Forecasts (ECMWF) analysis data for the grid point nearest the location of the aircraft profile and from temperature and humidity data taken with the Fiji ozonesonde profile 2 days earlier. The tropopause altitude (~16 km) was established from the ozone data from the on board lidar system [*Browell et al.*, this issue]. Because of the low-level convergence in the large-scale flow field, we also included vertical velocities in the initial conditions. A profile of vertical velocity from the vicinity of the SPCZ near Fiji was taken from the 1.5° × 1.5° resolution ECMWF field. The low-level upward motion induced by the convergence was 3–7 cm s^{-1}.

4.3. Cloud Characteristics

Figure 13 illustrates the evolution of the total hydrometeor field from the GCE model simulation of the SPCZ convection. Only shallow convection developed during the first hour of simulation, but by 1.5 hours the cloud had grown to ~6 km in depth (Figure 13a). Between 1.5 and 2 hours the cloud expanded considerably in horizontal dimension, reaching ~16 km altitude with an overshooting top to nearly 18 km (Figure 13b). The anvil top remained at ~16 km through 3 and 4 hours (e.g., Figure 13c) and reached its largest horizontal extent at 4.5 hours. After this time, the storm weakened considerably. The top of the simulated cloud compared favorably with the satellite-derived cloud top heights (Plate 2). The maximum vertical velocity within the cloud averaged ~15 m s^{-1}. The radar reflectivity computed from the model hydrometeor fields allows us to examine variations in strength of the convection

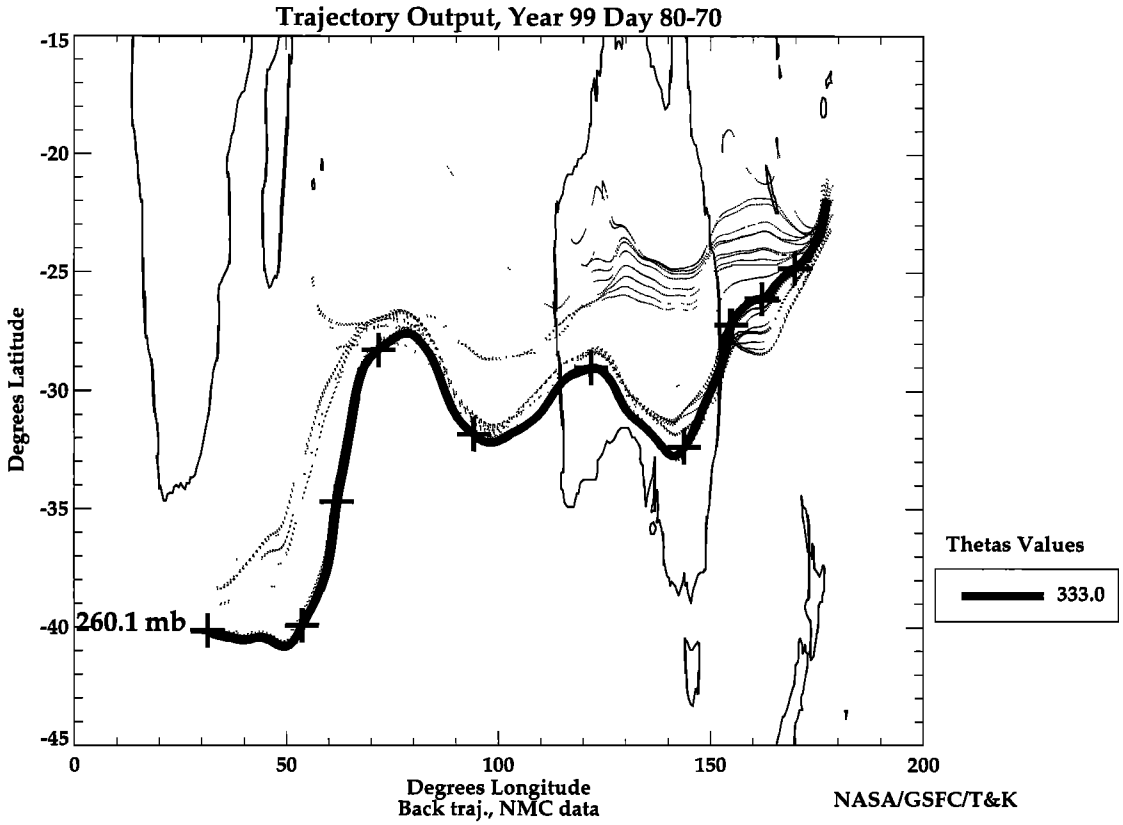

Figure 7. Ten-day back trajectory cluster on 333 K isentropic surface from location of ozone plume found in the 6.5–8 km layer on the spiral southwest of the SPCZ. The cluster consists of a central trajectory (shown with bold line) plus 24 additional trajectories begun at equally spaced locations within a 2.5° × 2.5° square around the central point. Large plus signs indicate parcel locations at 24-hour intervals.

throughout the simulation. Peaks in radar reflectivity of 60–70 dBZ were found in the lower troposphere between 2 and 4.5 hours. Reflectivity at DC-8 flight level (~11.3 km) was typically 45–55 dBZ, comparing favorably with the weather radar on board the DC-8, which showed strong reflectivities to the east of the aircraft during the southbound passage through the SPCZ.

4.4. Tracer Results

4.4.1. Convective Transport. Initial conditions for the chemical tracer calculations were derived primarily from the DC-8 profile northeast of the SPCZ. Profiles above the maximum altitude of the DC-8 were estimated by a variety of methods. Ozone data from the DIAL system, as well as from the March 18 Fiji ozonesonde (Figure 14) that is part of PEM-Tropics B [*Oltmans et al.*, this issue] and the Southern Hemisphere Additional Ozonesondes (SHADOZ (A. M. Thompson et al., The 1998–2000 SHADOZ tropical ozone climatology: Comparison with TOMS and surface measurements, submitted to *Journal of Geophysical Research*, 2001)) network, were used. NO_x in the lower stratosphere was estimated using NASA ER-2 aircraft measurements reported near Fiji by *Folkins et al.* [1997]. Nitric acid in the upper levels was estimated from the NO_y/O_3 ratio of 0.002 given by *Murphy et al.* [1993]. Values of H_2O_2, CH_3OOH, and H_2CO were taken from *Pickering et al.* [1993] 1-D photochemical model estimates for the Southern Hemisphere tropics. The very low values of CH_3I in the stratosphere were scaled against those for $CHBr_3$ (another marine tracer) given by *Schauffler et al.* [1999]. The initial data for nine species (O_3, CO, CH_3I, NO_x, HNO_3, H_2O_2, CH_3OOH, H_2CO, and SO_2) are summarized in Table 1 for the nine tracer layers of the model. The first three of these species are insoluble, with lifetimes considerably longer than a convective system, and can be used as tracers of convective transport and mixing. We simulate the transport of NO_x, primarily to enable the estimation of the contribution of lightning to the observed NO_x mixing ratios (see section 4.4.2). The latter five species are soluble, and we perform conserved tracer transport simulations to estimate the fraction of amounts of these species that are scavenged in the cloud.

Figures 15a and 15b present results for the ozone tracer at 2 and 4.5 hours in the simulation. Initially, ozone in the model at the DC-8 flight level during the SPCZ crossings (~11.3 km) was ~28 ppbv. The simulated convection transported lower values from the marine boundary layer to the middle and upper troposphere, so that 11-km mixing ratios decreased to ~11.5–13 ppbv. These values compare very well with the minimum (12–13 ppbv) recorded on the DC-8 during the northbound SPCZ crossing (Figure 9a). The model slightly overestimates the minimum ozone mixing ratio (10 ppbv) recorded on the southbound crossing. Ozone averaged over the cloud-perturbed region in the simulation was 15 ppbv at 2 hours and 17 ppbv at 4.5 hours, slightly overestimating the observed averages of 14.5 ppbv and 14 ppbv on the northbound and southbound crossings, respectively. The effect of the convection on

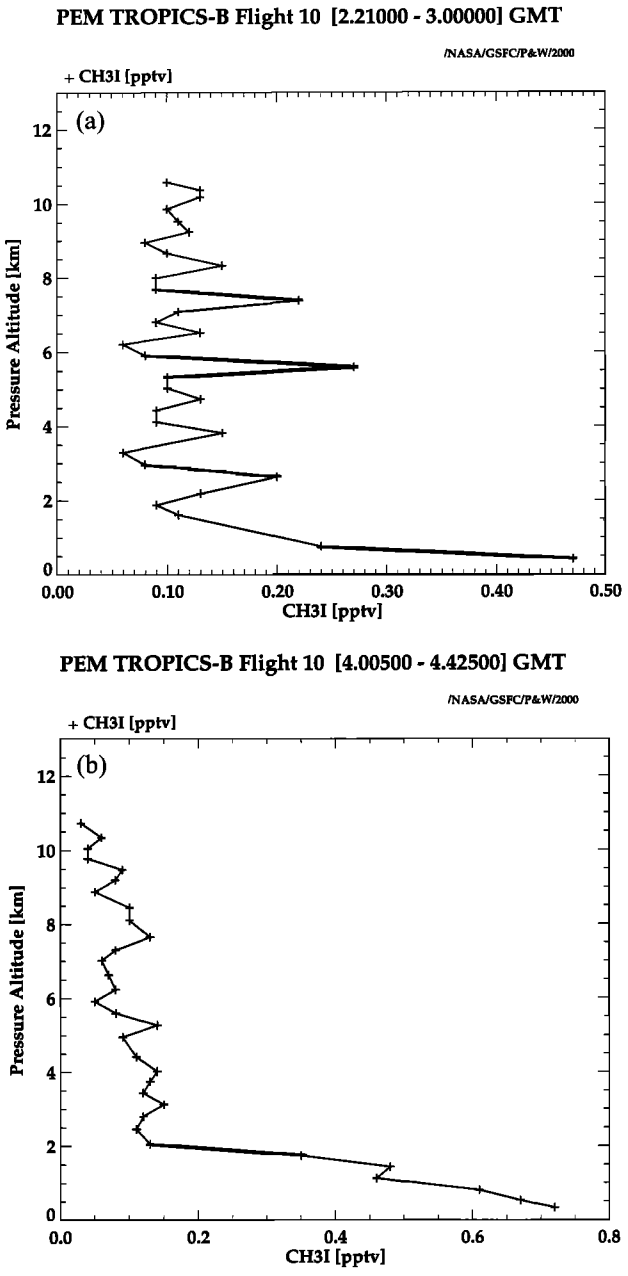

Figure 8. Profiles of CH_3I measured on the DC-8 during (a) spiral northeast of the SPCZ and (b) spiral southwest of the SPCZ.

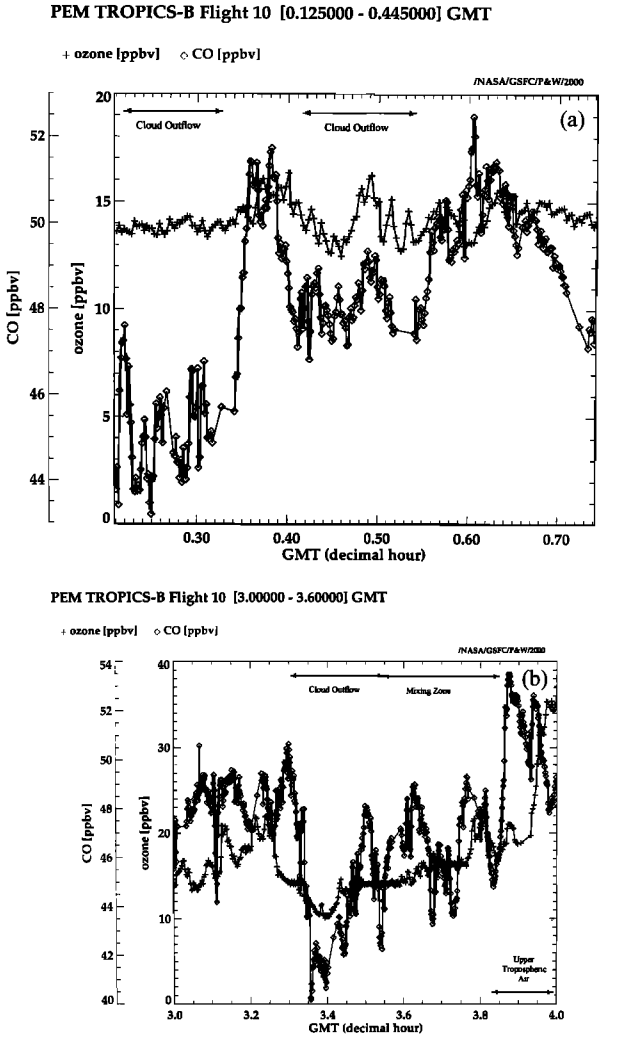

Figure 9. O_3 and CO measurements during (a) northbound and (b) southbound passages of the DC-8 through the SPCZ.

the O_3 distribution reached to 14–15 km. At 14 km the simulated O_3 mixing ratio at 2 hours decreased from an initial value of ~30 ppbv to 15–20 ppbv within the convective tower as a result of upward transport.

CH_3I mixing ratios in the model more than doubled at 11 km between the beginning of the convective simulation and 2 hours (Figure 16a). Maximum values at this level reached 0.26 pptv, which compares favorably with the maximum of 0.28 pptv observed in convective outflow on the northbound SPCZ crossing (Figure 10a), but underestimates the maximum values recorded during the southbound crossing (Figure 10b). The simulated maximum CH_3I mixing ratio at 11 km decreased to 0.22 pptv by 4.5 hours (Figure 16b). CH_3I averaged over the cloud-perturbed region in the simulation was 0.16 pptv at both 2 and 4.5 hours, compared with observed averages of 0.18 and 0.24 pptv on the northbound and southbound SPCZ crossings. There are four possible explanations for this underestimate: (1) a small quantity of boundary layer air from southwest of the SPCZ may have been entrained into the convection; (2) vertical velocities in the actual storm may have been slightly greater than produced in the model; (3) dilution of air in convective updraft cores may have been overestimated in the model; and (4) air parcels from very close to the sea surface (having CH_3I mixing ratios larger than the average for the 0–1 km layer used in the simulation) may have been transported to cloud outflow altitudes. Explanation 1 is unlikely because the ozone results do not suggest that this is the case. In fact, the ozone measurements suggest that slightly more low-ozone marine boundary layer from northeast of the SPCZ reached the upper troposphere than calculated by the model. Explanation 2 seems unlikely because the simulated vertical velocities are already relatively strong for a tropical marine convective system. Explanations 3 and 4 seem to be the most likely.

The convective transport calculations for O_3 and CH_3I show that the model produces reasonable estimates of changes in trace gas mixing ratios in the upper tropospheric cloud outflow region of the SPCZ. When we apply the model to NO_x and the

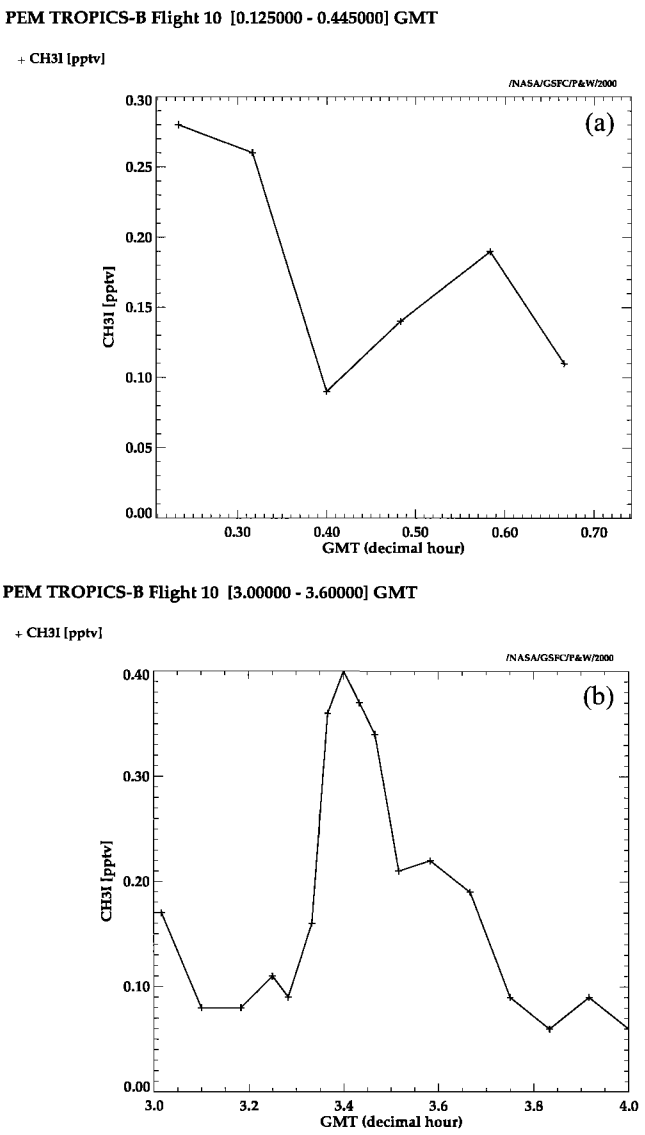

Figure 10. CH_3I measurements during (a) northbound and (b) southbound passages of the DC-8 through the SPCZ.

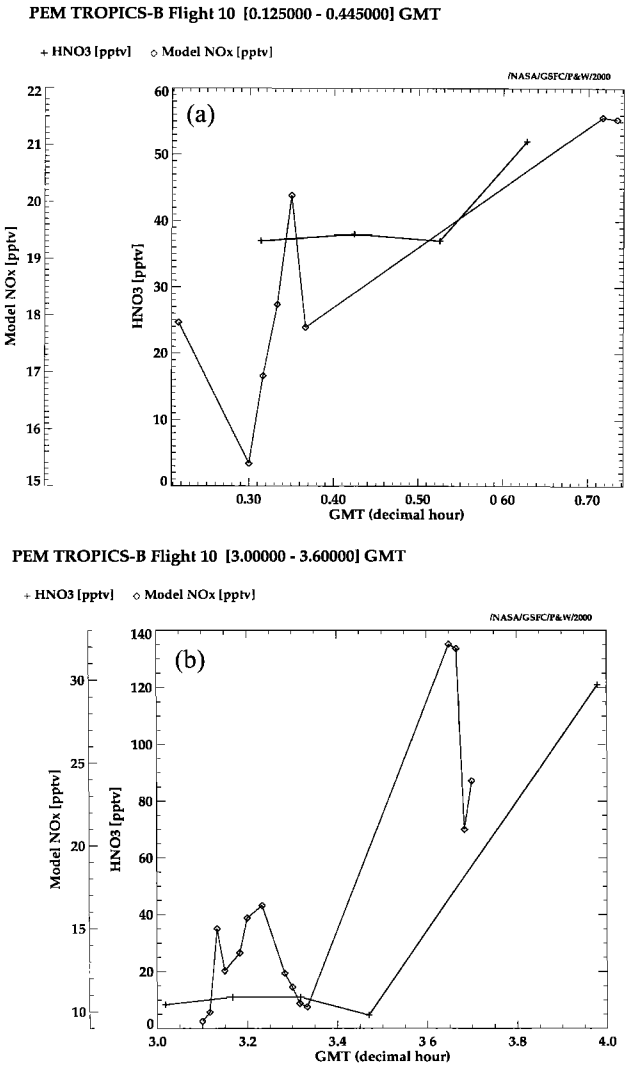

Figure 11. HNO_3 measurements and NO_x from the Langley/GIT box model for the periods of the (a) northbound and (b) southbound crossings of the SPCZ.

soluble species in the following subsections, we refer back to the findings concerning model transport characteristics presented here to support these analyses.

4.4.2. Lightning NO_x. Figures 17a and 17b present tracer transport results for NO_x with NO_x treated as a passive tracer with no sources or chemistry. Chemical loss is expected to be small over the short timescale of convective transport. However, in reality, NO_x could have been produced by lightning. At cloud outflow levels the model calculation represents NO_x mixing ratios with no production by lightning. Therefore we compare these values with those observed during the SPCZ crossing in order to make an estimate of the possible effect of lightning NO_x production by examining the difference between the two quantities. Observed NO_x (actually a box model estimate based on the observed NO) during the northbound SPCZ crossing was 16 to 20 pptv, while NO_x at flight level from the tracer transport calculations was ~5 pptv. Therefore the difference, 11 to 15 pptv, could be attributed to lightning NO_x production. This is a very small quantity, suggesting that the SPCZ cloud was not very electrically active. Unfortunately, the LIS did not have any overpasses in our study region during the period of the DC-8 flight. The DC-8 was equipped with a Stormscope, which detects electrical discharges of various types in clouds. The fraction of these discharges that are sufficiently energetic to produce NO_x is unknown. The Stormscope display on videotape was reviewed for the periods of the DC-8 approach to the SPCZ and the northbound crossing. During the DC-8 approach to the SPCZ from the south, 57 and 18 impulses were recorded to the left and right, respectively, of the DC-8 track, or an average of 2.2 discharges per minute. During the northbound SPCZ crossing, 37 and 10 impulses were recorded to the left and to the right, respectively, of the DC-8 track, or 3.8 discharges per minute. Therefore the majority of the electrical activity was to the west of the track. Easterly winds at flight level would have likely transported more lightning-generated NO_x away from the aircraft than toward it. However, if the upwind discharges had been productive of NO_x (e.g., 2×10^{20} to 1×10^{22} molecules NO per meter of flash channel [*Stith et al.*, 1999]), more than ~11 to 15 pptv should have been detected.

Unfortunately, NO_x data were not available from the DC-8

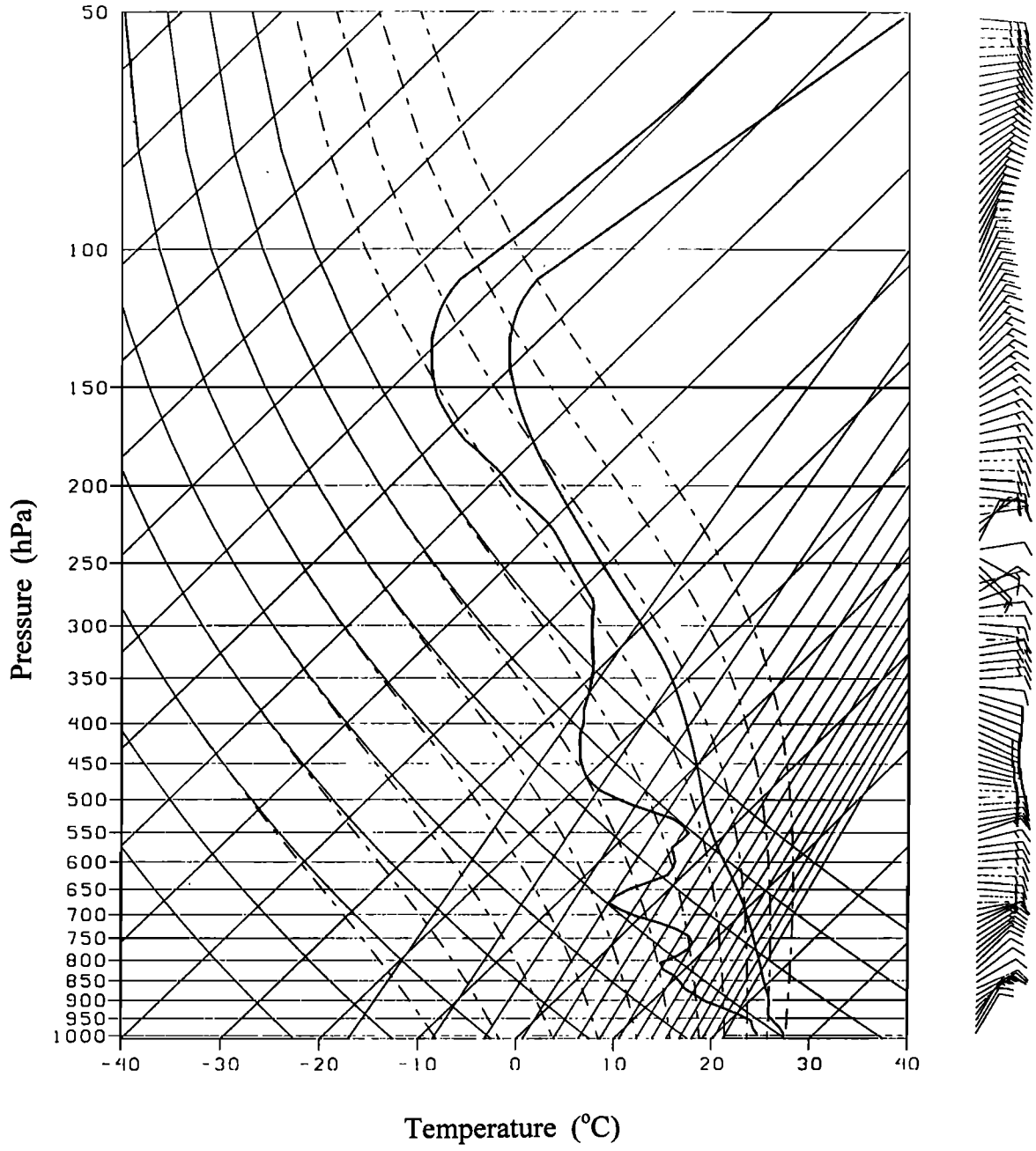

Figure 12. SkewT-logP diagram showing profiles of temperature, dew point, and winds used as initial conditions for the GCE model simulation of a representative cell in the SPCZ convective line.

during the southbound passage. The Stormscope recorded a much lesser number of discharges during this SPCZ crossing than it did during the northbound traverse. Only 15 discharges were noted to the left of the aircraft track, and 12 were noted to the right. Within the band of less deep convection to the north of the SPCZ, the DC-8 recorded some of the largest NO_x mixing ratios of the flight (up to 85 pptv). However, as the plane approached and passed through this region, only one discharge was noted. Perhaps this area of convection had been more electrically active earlier in the day.

4.4.3. Wet Scavenging of Soluble Species. Figure 18 shows our transport calculations for HNO_3 assuming no loss due to wet scavenging. At 4 hours, 30 min into the simulation the tracer results indicate that ~80 pptv HNO_3 would have been present at ~11 km if no scavenging occurred in the cloud. Over the simulation, HNO_3 typically ranged from 60 to 90 pptv. We compare these results with observations during the SPCZ crossing to estimate the fraction of HNO_3 removed in the cloud. During the southbound crossing, which had the stronger convective outflow signals in the chemical measurements (see section 3.2), observed HNO_3 reached a minimum of 5 pptv. We estimate the fraction of HNO_3 scavenged by computing (model—observed)/model. This estimate is representative of the strongest cloud outflow encountered by the aircraft during the SPCZ crossings. The outflow is a mixture of air parcels transported upward through the liquid portion of

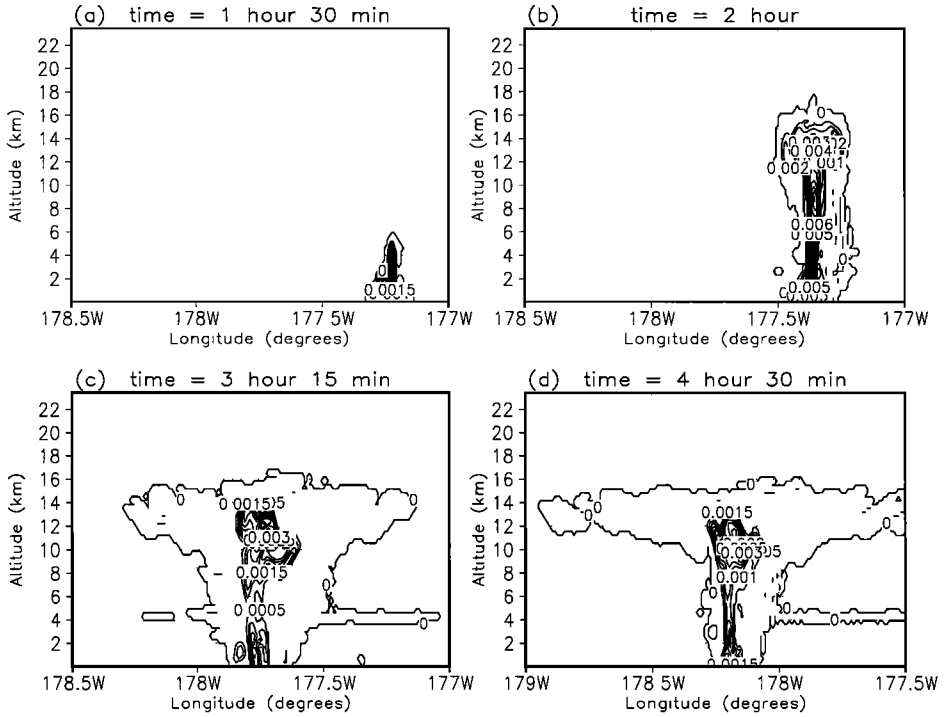

Figure 13. Evolution of the simulated cloud in terms of total hydrometeor mixing ratio g/g. Times shown are (a) 1.5, (b) 2, (c) 3.25, and (d) 4.5 hours.

the cloud and air parcels flowing through the upper tropospheric (primarily ice) part of the cloud. Therefore it is likely that these estimates will not be as large as if only air that had passed through the liquid portion of the cloud had been sampled. We obtain an estimate of 0.94 as the fraction of HNO_3 scavenged, not unexpected because HNO_3 is extremely soluble. Some uncertainty in this estimate is due to the very low

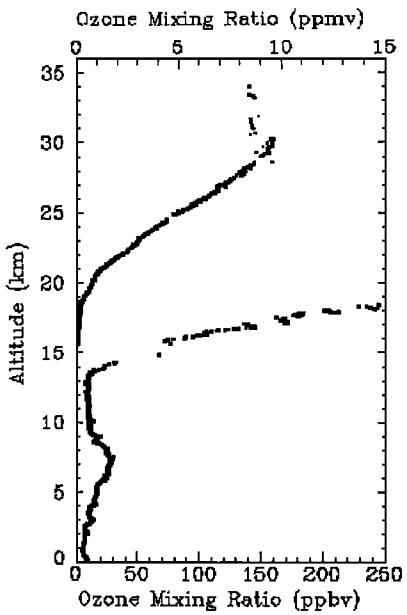

Figure 14. Ozone profile from ozonesonde observation taken at Suva, Fiji, at 2134 UT March 18, 1999.

Table 1. Initial Conditions for Tracer Transport Calculations

Altitude, km	O_3,ppbv	CO,ppbv	NO_x,pptv
0–1	6.0	41	2.3
1–2	7.2	39.5	2.1
2–4	12.7	42	2.1
4–6	14.3	46.7	2.8
6–8	15.1	45	5.4
8–11	14.5	48.5	10.3
11–16.	28	48	18
16–18	150	30	100
18–23	1000	25	400
Altitude, km	CH_3I, pptv	H_2O_2, pptv	CH_3OOH, pptv
0–1	0.34	1400	390
1–2	0.15	1255	335
2–4	0.20	735	245
4–6	0.12	475	145
6–8	0.11	270	100
8–11	0.11	155	100
11–16	0.11	155	100
16–18	0.01	50	20
18–23	0.01	5	1
Altitude, km	HNO_3, pptv	H_2CO, pptv	SO_2, pptv
0–1	145	470	21
1–2	59	320	46
2–4	49	225	40
4–6	39	170	46
6–8	23	100	36
8–11	34	170	26
11–16	34	90	26
16–18	300	10	20
18–23	2000	1	10

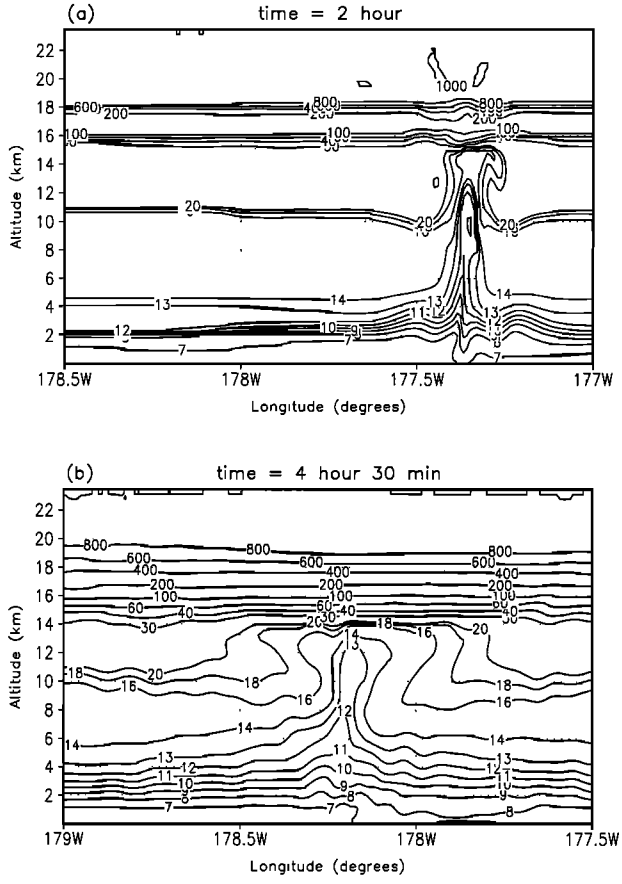

Figure 15. Ozone tracer field from 2-D GCE model at (a) 2 hours and (b) 4.5 hours into the simulation of SPCZ convection of March 20–21, 1999.

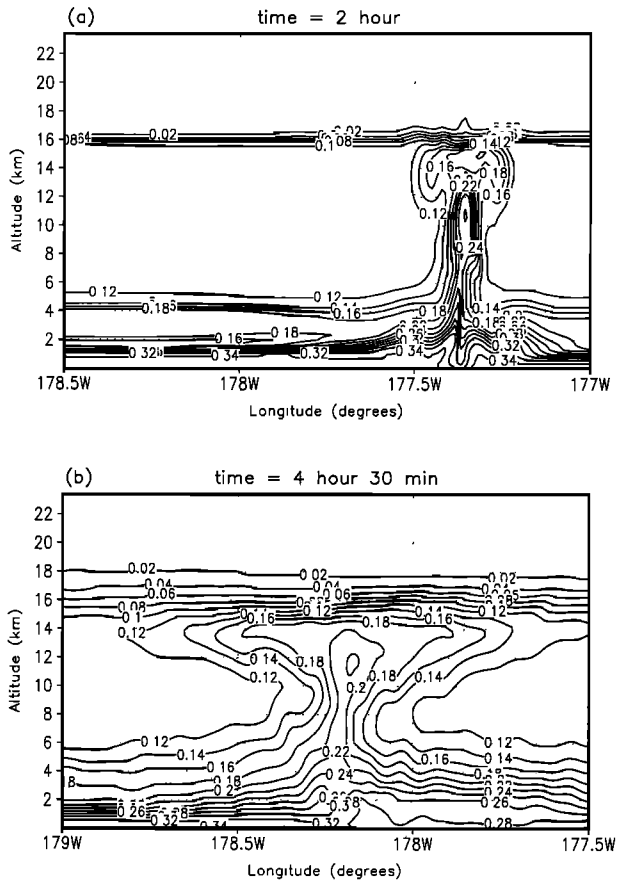

Figure 16. Same as Figure 15, except for CH_3I.

mixing ratios in the outflow (i.e., at or below the instrument detection limit). Somewhat smaller fractions scavenged (~0.7) are estimated for the outer part of the cloud anvil. The cloud model output at ~11 km indicates that the hydrometeors at this altitude were almost all in the form of snow, graupel, or cloud ice. Therefore these results suggest that HNO_3 either was retained by the hydrometeors during the freezing process or uptake onto the ice particles occurred.

Similar calculations were performed for H_2O_2, CH_3OOH, H_2CO, and SO_2 (see Table 2). A large fraction scavenged (0.91) was obtained for H_2O_2, which is also very soluble. We obtain a considerably lesser fraction for CH_3OOH (0.48) which is much less soluble. For H_2CO and SO_2 we obtain intermediate values of the fraction scavenged, 0.78 and 0.66, respectively. Dilution during convective transport may have been overestimated in the model (see section 4.4.1). With lesser dilution our calculations of the fractions scavenged would be slightly larger. Comparison of these results with the simulation of wet removal by *Mari et al.* [2000] for another tropical convective storm suggests that there was a very high rate of conversion of cloud water to precipitation in the SPCZ convection. Indeed, our GCE model simulation shows very large radar reflectivity values indicative of large precipitation rates.

5. Discussion

5.1. Photochemical Ozone Production

We have demonstrated that tropical marine boundary layer air from northeast of the SPCZ entered the convection and was transported in updrafts to the anvil. In the anvil the outflow from the convective cells was transported in the easterly winds to the southwestern edge of the SPCZ cloud band. There it mixed with subtropical air containing considerably larger mixing ratios of O_3 and NO_x being transported to the SPCZ region from the south and west. We have examined the instantaneous rates of photochemical ozone production and loss calculated for air northeast and southwest of the SPCZ, in the convective outflow, and in the region of mixing on the southwest edge of cloud band. We use values of ozone production and loss (see Table 3) computed with the NASA Langley—Georgia Tech box model [*Davis et al.*, 1996b; *Crawford et al.*, 1997]. The model uses the 1-min merged data set produced at Harvard as input. Values of ozone, CO, NO, dew point, and $j(NO_2)$ are required in the calculation, and where possible, the model is also constrained by observed H_2O_2, CH_3OOH, HNO_3, and PAN. Measured hydrocarbons are used where available. Interpolated hydrocarbon mixing ratios are used in short gaps, and regional median values are used for the appropriate altitude range in longer hydrocarbon data gaps.

A substantial rate of net ozone destruction (-7.80×10^5 molecules cm^{-3} s^{-1}) was computed in the very low NO (~2 pptv) boundary layer air on the northeast side of the SPCZ. At 11.3 km there was net ozone production (5.72×10^4 molecules cm^{-3} s^{-1}) in air undisturbed by convection (NO = 16 pptv). At the same altitude in convective outflow, net ozone production was only 2.18×10^4 molecules cm^{-3} s^{-1} because convection brought up low-NO (~8 pptv) boundary layer air, reducing the ozone producing capability by ~60%. At 11.3 km on the south-

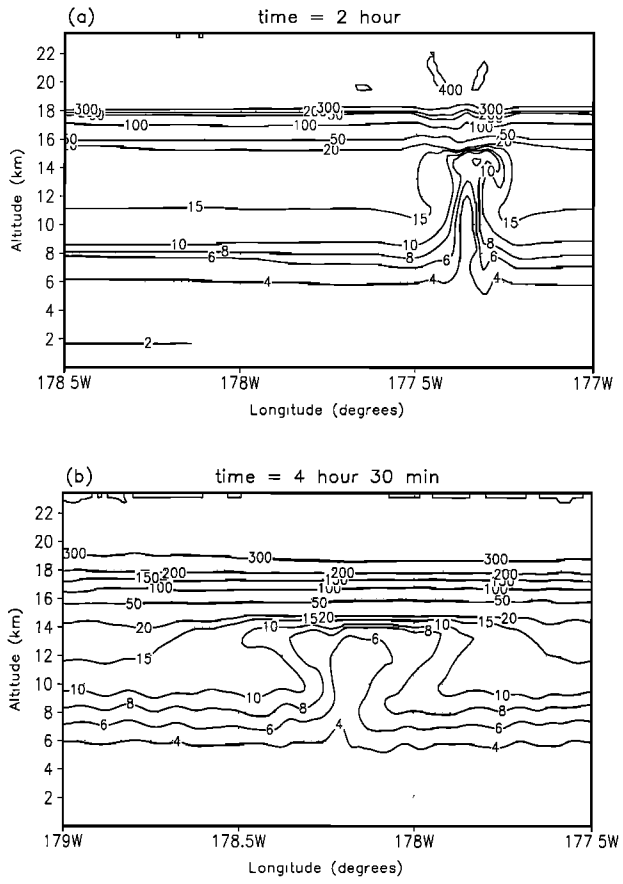

Figure 17. Same as Figure 16, except for NO_x.

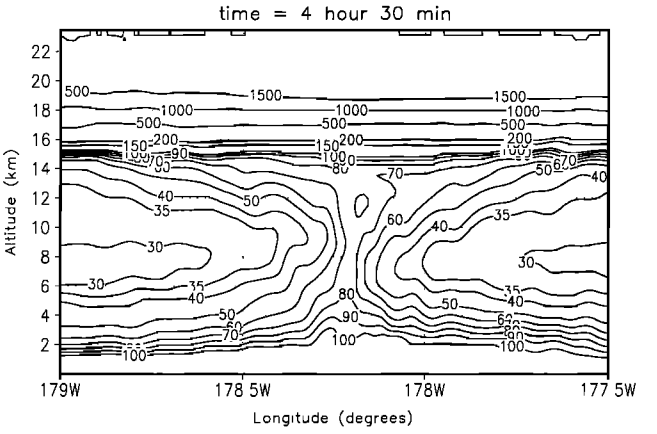

Figure 18. Nitric acid tracer (no scavenging) field from the 2-D GCE model at 4.5 hours into the simulation of SPCZ convection of March 20–21, 1999.

west side of the SPCZ an enhanced NO layer (~47 pptv) led to a net ozone production rate of 1.23×10^5 molecules cm^{-3} s^{-1}. At the southwest edge of the cloud system, SPCZ convective outflow mixed with this enhanced NO layer, resulting in net ozone production rates intermediate between those of the two air masses (e.g., 6.98×10^4 molecules cm^{-3} s^{-1} for a point just outside the cloud with NO mixing ratio of ~24 pptv).

5.2. Comparison With Other Tropical Convective Systems

Thompson et al. [1997] summarized several analyses and simulations of tropical convective events in relation to ozone production. Over continental regions polluted with either urban or biomass burning emissions, deep convection led to a factor of 3–4 increase in upper tropospheric net ozone production downwind when the upper troposphere already contained outflow from previous upstream convection [e.g., *Pickering et al.*, 1996]. In a pristine upper troposphere much larger ozone production increases are estimated. Calculations for continental cases contrast with those performed for a marine convective event that occurred between Australia and New Guinea during STEP/EMEX [*Pickering et al.*, 1993]. In this case, convection reduced net ozone production in the 14.5 to 17 km outflow layer by 15–20% due to the upward transport of low-NO marine boundary layer air. The PEM-Tropics B SPCZ case analyzed here caused a ~60% reduction in net ozone production in cloud outflow. Maximum vertical velocities in the STEP/EMEX convection were relatively weak, so the amount of low-NO air reaching outflow levels was relatively small. In addition, the initial vertical gradients of trace species in STEP/EMEX were minimal due to frequent prior convection. Therefore it is not surprising that the SPCZ convection had a larger effect on upper tropospheric net ozone production.

Kley et al. [1996] reported ozonesonde observations during CEPEX, which was conducted March 7 to April 7, 1993, in the tropical Pacific from 150°E to 160°W at 2°S. The ozonesonde data show clear evidence of the redistribution of ozone by deep convection (ozone mixing ratios as low as 5 ppbv in the upper troposphere and values as large as 15 ppbv transported to the marine boundary layer). *Wang and Prinn* [2000] used a cloud-resolving model with chemistry to simulate the March 8, 1993, CEPEX convective event. The lowest ozone mixing ratios computed in the upper troposphere were ~2 ppbv, an 80% decrease from the preconvective conditions. This ozone mixing ratio is considerably smaller than the minimum value found in the SPCZ case analyzed here (~10 ppbv). In another CEPEX event, *Wang et al.* [1995] simulated tracer transport and estimated a minimum ozone value of 9 ppbv in the cloud anvil, which closely compares with that observed in the SPCZ.

We noted only very small enhancements of upper tropospheric NO_x possibly due to lightning during one of the SPCZ crossings. However, the Stormscope on board the DC-8 recorded an average of 2–3 discharges per minute as the plane approached and passed through the convective system. *Pickering et al.* [1998] simulated lightning NO production in a squall line that occurred during TOGA-COARE near the Solomon Islands in the tropical Pacific. When the model parameterization was adjusted to produce the measured flash rates of 1–2 per minute, it yielded maximum NO_x mixing ratios in the anvil of 0.7–0.9 ppbv. These values are similar to those reported by

Table 2. Wet Scavenging of Soluble Species in SPCZ Convection

Species	Tracer Calculation Without Scavenging at 11 km, pptv	Measurement in Maximum Outflow, pptv	Fraction Scavenged
HNO_3	80	5	0.94
H_2O_2	800	70	0.91
CH_3OOH	250	130	0.48
H_2CO	300	65	0.78
SO_2	35	12	0.66

Table 3. Net Ozone Production Computed With Langley/GIT Box Model

Air Mass	Local Time	[NO], pptv	$[O_3]$, ppbv	Instantaneous Net O_3 Production, molecules cm^{-3} s^{-1}	24-hour Average Net O_3 Production, molecules cm^{-3} s^{-1}
Boundary layer NE of SPCZ	1418	2	5	-7.80×10^5	-2.59×10^5
Upper troposphere NE of SPCZ	1508	16	28	5.72×10^4	2.33×10^4
Upper tropospheric SPCZ outflow	1520	8	10	2.18×10^4	1.39×10^4
Upper troposphere SW of SPCZ	1605	47	55	1.23×10^5	5.53×10^4
Upper tropospheric mixing region	1542	24	35	6.98×10^4	3.16×10^4

Chameides et al. [1987] for anvil penetrations of two tropical convective cells over the North Pacific. Therefore it seems likely that most of the SPCZ Stormscope signals were from discharges not sufficiently energetic to produce significant quantities of NO.

6. Summary

We have analyzed and simulated with a cloud-resolved model trace gas transport and scavenging in SPCZ deep convection observed during the PEM-Tropics B experiment. We have examined in detail the structure of convective mixing, the production of lightning NO, and the wet scavenging of several soluble species, which are three of the most uncertain processes in regional and global chemical transport models (CTMs). Wind fields from a 2-D cloud-resolving model were used with tracers to diagnose transport characteristics, lightning NO production, and wet scavenging. The conclusions are as follows:

1. For transport, from the model and the observations, we conclude that air in deep convective outflow sampled by the DC-8 was mostly derived from the marine boundary layer in the tropical air mass northeast of the SPCZ. It appeared that very little boundary layer air from southwest of the SPCZ was entrained into the convection. Therefore, at low levels, the SPCZ acts as a barrier to mixing. However, because the SPCZ convection changes position from day to day and is more active on some days than others, this low-level barrier is spatially and temporally transient. The observations suggest that most of the mixing of the tropical air from northeast of the SPCZ with Southern Hemispheric subtropical air from southwest of the SPCZ occurred after the tropical air had been processed by the convective cloud. This mixing took place in the upper troposphere on the southwest edge of the convective cloud band. At the portion of SPCZ northwest of Fiji the tropical air north of the SPCZ had a Northern Hemispheric origin. Therefore, during PEM-Tropics B, it is likely that this part of the SPCZ served to mix air from the two hemispheres.

2. For lightning, by comparing model-calculated tracer transport of NO_x to observed outflow levels, we conclude that very little NO appears to have been produced by lightning within the SPCZ convection, despite vertical velocities that were fairly strong for a tropical marine system. However, during the northbound passage the aircraft was not at the best location to capture maximum outflow, and NO data were not collected during most of the southbound passage.

3. For wet scavenging, tracer calculations for the soluble species were compared with the outflow measurements to estimate fractions of species which had been removed by wet scavenging during transport through the cloud. Very large fractions were computed for the most soluble species (~90% for HNO_3 and H_2O_2) and lesser fractions (48–78%) for less soluble species (CH_3OOH, SO_2, and H_2CO). Convective transport of low-NO marine boundary layer air to the upper troposphere reduced net ozone production in this region by ~60%. This air mixed with higher-NO air arriving from the west at these altitudes, resulting in air parcels with ozone production rates intermediate between the preconvective rates on either side of the SPCZ. Therefore the SPCZ modifies the ozone-producing capacity of the South Pacific troposphere.

Comparison of parameterized convective mixing, lightning NO production, and wet scavenging from regional and global model simulations of the March 20–21, 1999, SPCZ event with the observational and cloud-resolving model results presented here serves as a means of evaluating and refining such parameterizations. Therefore, if parameterization improvements result from the comparisons, detailed process analyses for specific events such as that presented here will likely aid in reducing uncertainties and inaccuracies in regional and global CTMs.

Acknowledgments. This work was supported by the NASA Tropospheric Chemistry Program (to A.M.T.) and under NASA EOS Interdisciplinary Science Investigations (to K.E.P. and to A. Dessler). We thank Wei-Kuo Tao for use of the GCE model and Gera Stenchikov and Aiwu Li for assistance with the cloud modeling effort. We also thank Henry Fuelberg and Joe Maloney of Florida State University for providing the ECMWF fields.

References

Browell, E. V., et al., Large-scale air mass characteristics observed over the remote tropical Pacific Ocean during March–April 1999: Results from PEM-Tropics B field experiment, *J. Geophys. Res.*, this issue.

Chameides, W. L., D. D. Davis, J. Bradshaw, M. Rodgers, S. Sandholm, and D. B. Bai, An estimate of NO_x production rate in electrified clouds based on NO observations from the GTE/CITE 1 fall 1983 field operation, *J. Geophys. Res.*, *92*, 2153–2156, 1987.

Christian, H. J., and J. Latham, Satellite measurements of global lightning, *Q. J. R. Meteorol. Soc.*, *124*, 1771–1773, 1998.

Christian, H. J., et al., The Lightning Imaging Sensor, *NASA Conf. Publ.*, *CP-1999-209261*, 746–749, 1999.

Climate Prediction Center, Climate Diagnostics Bulletin, *99/3*, Natl. Cent. For Environ. Predict., Natl. Oceanic and Atmos. Admin., Camp Springs, Md., 1999.

Cohan, D. S., M. G. Schultz, D. J. Jacob, B. G. Heikes, and D. R. Blake, Convective injection and photochemical decay of peroxides in the tropical upper troposphere: Methyl iodide as a tracer of marine convection, *J. Geophys. Res.*, *104*, 5717–5724, 1999.

Crawford, J., et al., An assessment of ozone photochemistry in the extra-

tropical western North Pacific: Impact of continental outflow during the late winter/early spring, *J. Geophys. Res.*, *102*, 28,469–28,488, 1997.

Davis, D. D., J. Crawford, S. Liu, S. McKeen, A. Bandy, D. Thornton, F. Rowland, and D. Blake, Potential impact of iodine on tropospheric levels of ozone and other critical oxidants, *J. Geophys. Res.*, *101*, 2135–2147, 1996a.

Davis, D. D., et al., Assessment of ozone photochemistry in the western North Pacific as inferred from PEM-West A observations during the fall 1991, *J. Geophys. Res.*, *101*, 2111–2134, 1996b.

DeCaria, A., K. Pickering, G. Stenchikov, J. Scala, J. Stith, J. Dye, B. Ridley, and P. Laroche, A cloud-scale model study of lightning-generated NO_x in an individual thunderstorm during STERAO-A, *J. Geophys. Res.*, *105*, 11,601–11,616, 2000.

Dickerson, R. R., et al., Thunderstorms: An important mechanism in the transport of air pollutants, *Science*, *235*, 460–465, 1987.

Folkins, I., R. Chatfield, D. Baumgardner, and M. Proffitt, Biomass burning and deep convection in southeastern Asia: Results from ASHOE/MAESA, *J. Geophys. Res.*, *102*, 13,291–13,299, 1997.

Fuelberg, H. E., R. E. Newell, D. J. Westberg, J. C. Maloney, J. R. Hannan, B. D. Martin, M. A. Avery, and Y. Zhu, A meteorological overview of the second Pacific Exploratory Mission in the tropics, *J. Geophys. Res.*, this issue.

Gregory, G. L., et al., Chemical characteristics of Pacific tropospheric air in the region of the Intertropical Convergence Zone and South Pacific Convergence Zone, *J. Geophys. Res.*, *104*, 5677–5698, 1999.

Huang, H.-J., and D. G. Vincent, Major changes in circulation features over the South Pacific during FGGE, 10–27 January 1979, *Mon. Weather Rev.*, *111*, 1611–1618, 1983.

Kessler, E., *On the Distribution and Continuity of Water Substance in Atmospheric Circulations, Meteorol. Monogr.*, vol. 10, Am. Meteorol. Soc., Boston, Mass., 1969.

Kiladis, G. N., H. von Storch, and H. van Loon, Origin of the South Pacific Convergence Zone, *J. Clim.*, *2*, 1185–1195, 1989.

Kley, D., P. J. Crutzen, H. G. J. Smit, H. Vommel, S. J. Oltmans, H. Grassl, and V. Ramanathan, Observations of near-zero ozone concentrations over the convective Pacific: Effects on air chemistry, *Science*, *274*, 230–233, 1996.

Lelieveld, J., and P. J. Crutzen, Role of deep cloud convection in the ozone budget of the troposphere, *Science*, *264*, 1759–1761, 1994.

Lin, Y.-L., R. D. Farley, and H. D. Orville, Bulk parameterization of the snow field in a cloud model, *J. Clim. Appl. Meteorol.*, *22*, 1065–1092, 1983.

Lindzen, R. S., and S. Nigam, On the role of sea surface temperature gradients in forcing low-level winds and convergence in the tropics, *J. Atmos. Sci.*, *44*, 2418–2436, 1987.

Mari, C., D. J. Jacob, and P. Bechtold, Transport and scavenging of soluble gases in a deep convective cloud, *J. Geophys. Res.*, *105*, 22,255–22,268, 2000.

Murphy, D. M., D. W. Fahey, M. H. Proffitt, S. C. Liu, K. R. Chan, C. S. Eubank, S. R. Kawa, and K. K. Kelly, Reactive nitrogen and its correlation with ozone in the lower stratosphere and upper troposphere, *J. Geophys. Res.*, *98*, 8751–8773, 1993.

Oltmans, S. J., et al., Ozone in the Pacific tropical troposphere from ozonesonde observations, *J. Geophys. Res.*, this issue.

Pickering, K. E., A. M. Thompson, R. R. Dickerson, W. T. Luke, and D. P. McNamara, Model calculations of tropospheric ozone production potential following observed convective events, *J. Geophys. Res.*, *95*, 14,049–14,062, 1990.

Pickering, K. E., A. M. Thompson, J. R. Scala, W.-K. Tao, J. Simpson, and M. Garstang, Photochemical ozone production in tropical squall line convection during NASA/GTE/ABLE-2A, *J. Geophys. Res.*, *96*, 3099–3114, 1991.

Pickering, K. E., A. M. Thompson, J. Scala, W.-K. Tao, R. R. Dickerson, and J. Simpson, Free tropospheric ozone production following entrainment of urban plumes into deep convection, *J. Geophys. Res.*, *97*, 17,985–18,000, 1992.

Pickering, K. E., A. M. Thompson, W.-K. Tao, and T. L. Kucsera, Upper tropospheric ozone production following mesoscale convection during STEP/EMEX, *J. Geophys. Res.*, *98*, 8737–8749, 1993.

Pickering, K. E., et al., Convective transport of biomass burning emissions over Brazil during TRACE-A, *J. Geophys. Res.*, *101*, 23,993–24,012, 1996.

Pickering, K. E., Y. Wang, W.-K. Tao, C. Price, and J.-F. Mueller, Vertical distributions of lightning NO_x for use in regional and global chemical transport models, *J. Geophys. Res.*, *103*, 31,203–31,216, 1998.

Raper, J. L., M. M. Kleb, D. J. Jacob, D. D. Davis, R. E. Newell, H. E. Fuelberg, R. J. Bendura, J. M. Hoell, and R. J. McNeal, Pacific Exploratory Mission in the tropical Pacific: PEM-Tropics B, March–April 1999, *J. Geophys. Res.*, this issue.

Scala, J. R., et al., Cloud draft structure and trace gas transport, *J. Geophys. Res.*, *95*, 17,015–17,030, 1990.

Schauffler, S. M., E. L. Atlas, D. R. Blake, F. Flocke, R. A. Lueb, J. M. Lee-Taylor, V. Stroud, and W. Travnicek, Distributions of brominated organic compounds in the troposphere and lower stratosphere, *J. Geophys. Res.*, *104*, 21,513–21,535, 1999.

Stenchikov, G., R. Dickerson, K. Pickering, W. Ellis Jr., B. Doddridge, S. Kondragunta, O. Poulida, J. Scala, and W.-K. Tao, Stratosphere-troposphere exchange in a midlatitude mesoscale convective complex, 2, Numerical simulations, *J. Geophys. Res.*, *101*, 6837–6851, 1996.

Stith, J., J. Dye, B. Ridley, P. Laroche, E. Defer, K. Baumann, G. Huebler, R. Zerr, and M. Venticinque, NO signatures from lightning strikes, *J. Geophys. Res.*, *104*, 16,081–16,089, 1999.

Streten, N. A., Some characteristics of satellite-observed bands of persistent cloudiness over the Southern Hemisphere, *Mon. Weather Rev.*, *101*, 486–495, 1973.

Tao, W.-K., and J. Simpson, The Goddard Cumulus Ensemble Model, part I, Model description, *Terr. Atmos. Oceanic Sci.*, *4*, 35–72, 1993.

Tao, W.-K., J. Simpson, C.-H. Sui, B. Ferrier, S. Lang, J. Scala, M.-D. Chou, and K. Pickering, Heating, moisture, and water budgets of tropical and midlatitude squall lines: Comparisons and sensitivity to longwave radiation, *J. Atmos. Sci.*, *50*, 673–690, 1993.

Thompson, A. M., W.-K. Tao, K. E. Pickering, J. R. Scala, and J. Simpson, Tropical deep convection and ozone formation, *Bull. Am. Meteorol. Soc.*, *78*, 1043–1054, 1997.

Thompson, A. M., H. B. Singh, and H. Schlager, Introduction to special section: Subsonic Assessment Ozone and Nitrogen Oxide Experiment (SONEX) and Pollution From Aircraft Emissions in the North Atlantic Flight Corridor (POLINAT 2), *J. Geophys. Res.*, *105*, 3595–3603, 2000.

Trenberth, K. E., Spatial and temporal variations of the southern oscillation, *Q. J. R. Meteorol. Soc.*, *102*, 639–653, 1976.

Trenberth, K. E., General characteristics of the El Nino-Southern Oscillation, in *Teleconnections Linking Worldwide Climate Anomalies*, edited by M. Glantz, R. W. Katz, and N. Nicholls, pp. 13–41, Cambridge Univ. Press, New York, 1991.

Vincent, D. G., The South Pacific Convergence Zone (SPCZ): A review, *Mon. Weather Rev.*, *122*, 1949–1970, 1994.

Wang, C., and R. G. Prinn, On the roles of deep convective clouds in tropospheric chemistry, *J. Geophys. Res.*, *105*, 22,269–22,298, 2000.

Wang, C., P. J. Crutzen, V. Ramanathan, and S. F. Williams, The role of a deep convective storm over the tropical Pacific Ocean in the redistribution of atmospheric chemical species, *J. Geophys. Res.*, *100*, 11,509–11,516, 1995.

M. A. Avery, J. H. Crawford, and G. W. Sachse, NASA Langley Research Center, Hampton, VA 23681, USA.

D. R. Blake, Department of Chemistry, University of California, Irvine, CA 92717, USA.

A. J. DeCaria, Department of Earth Sciences, Millersville University, Millersville, PA 17551, USA.

B. G. Heikes, Graduate School of Oceanography, University of Rhode Island, Narragansett, RI 02882, USA.

H. Kim and K. E. Pickering, Department of Meteorology, University of Maryland, College Park, MD 20742-2425, USA. (pickering@metosrv2.umd.edu)

T. L. Kucsera and J. C. Witte, SSAI, NASA Goddard Space Flight Center, Greenbelt, MD 20771, USA.

L. Pfister, NASA Ames Research Center, Moffitt Field, CA 94035, USA.

S. T. Sandholm, School of Earth and Atmospheric Sciences, Georgia Institute of Technology, Atlanta, GA 30332, USA.

R. W. Talbot, Institute for Earth, Oceans, and Space, University of New Hampshire, Durham, NH 03824, USA.

A. M. Thompson, Laboratory for Atmospheres, NASA Goddard Space Flight Center, Greenbelt, MD 20771, USA.

(Received January 4, 2001; revised May 4, 2001;
accepted May 8, 2001.)